Desalination and Water Treatment
www.deswater.com

doi: 10.1080/19443994.2013.771287

51 (2013) 6871–6881
October

Taylor & Francis
Taylor & Francis Group

Comparison of new biosorbents based on chemically modified *Lagenaria vulgaris* shell

Danijela V. Bojić, Marjan S. Ranđelović*, Aleksandra R. Zarubica, Jelena Z. Mitrović, Miljana D. Radović, Milovan M. Purenović, Aleksandar Lj. Bojić

Faculty of Science and Mathematics, Department of Chemistry, University of Niš, 33 Višegradska Street, Niš 18000, Serbia
Tel./Fax: +381 18 533014; email: marjanra@pmf.ni.ac.rs

Received 21 November 2012; Accepted 19 January 2013

ABSTRACT

Sorption characteristics of three *Lagenaria vulgaris*-based biosorbents: raw biomass (*r*LVB), acid–base-activated biomass (*a*LVB) and sulfuric acid-treated biomass (*cc*LVB), were compared as a function of contact time, initial methylene blue concentration, and initial pH, in order to evaluate the effect of chemical modifications. The adsorption studies of raw and chemically modified *L. vulgaris* biomass were compared in batch mode. The Fourier transform Infrared spectroscopy (FTIR) results of biosorbents' characterization showed presence of different functional groups which can be responsible for sorption of MB from aqueous solutions. Moreover, FTIR analysis reveals that acid–base activation of raw biomaterial resulted in hydrolysis of esters providing more reactive sites ($-COO^-$), while sulfuric acid-treatment method introduced new functional groups such as $-SO_3^-$. Surface functional groups containing oxygen, such as carboxylic, lactonic, and phenolic, are quantified using the Boehm's method. The kinetics of MB biosorption were found to follow a pseudo-second-order kinetics in all cases, while experimental equilibrium data were fitted to Freundlich, Langmuir, and Dubinin–Radushkevich isotherms by linear regression method. *Langmuir model* provides the *best fitting*. The MB biosorption capacity and uptake kinetics are greatly improved by chemical modification of the biomass. Effectiveness of examined biosorbents in MB removal from aqueous solutions can be put in the following order: *r*LVB < *a*LVB < *cc*LVB.

Keywords: Biosorption; *Lagenaria vulgaris*; Chemical modification; Mehylene blue; Kinetics; Isotherms

1. Introduction

Environmental contamination and deterioration of ecosystems are a major concern being faced by the modern society. Due to the rapid technological development, a large amount of industrial, agricultural, and domestic wastes are discharged in the environment. Usually, these discharges are directed to the nearest water recipient such as rivers, lakes, and seas. In accordance with this, the increasing need for clean drinking water, as well as strict requirements regarding the quality of waste waters, led to the development of new low-cost materials and corresponding alternative technologies for water purification. One of

*Corresponding author.

the most commonly used techniques for water purification is the adsorption process on natural or synthetic adsorbents. In this respect, a number of materials have been investigated, such as: silicates (clays and clay minerals, sand, zeolites etc.) in their natural or modified form [1–4], oxides [5], activated carbons [6–8], carbon nanotubes (CNT) [9], ion-exchanging resins [10], etc. In recent years, adsorption on biomass and waste materials from agriculture has attracted great attention of scientists due to wide availability of biomaterials, their low-cost and potentially high efficiency in the removal of pollutants from water. Biosorption involves the removal of pollutants from aqueous solutions by using live or dead biomass or their derivatives. Due to high biodiversity on the Earth, a large number of biomaterials for the removal of heavy metals, dyes, and other nonbiodegradable organic and inorganic pollutants have been examined so far, including rice husk [11], sawdust [12], peanut shell [13], yellow passion fruit waste [14], banana pith [15], aquatic plants [16,17], free and immobilized micro-organisms [18], etc.

Lagenaria vulgaris is an annual herbaceous plant, whose fruit shell is composed mostly of cellulose and lignin [19]. It was traditionally used for capturing and storing water, because of its characteristic shape. Moreover, *L. vulgaris* is fast-growing and available in large quantity. According to the author's best knowledge, the fruit shell of this plant has not been examined and used as biosorbent for water purification earlier, in spite of its good adsorption characteristics. For experimental purposes, three types of biosorbents based on *L. vulgaris* shell were prepared: (1) raw material—*r*LVB; (2) acid–base-activated material—*a*LVB, and (3) chemically modified material by sulfuric acid treatment—*cc*LVB biosorbent. All materials were characterized in detail by Fourier transform infrared spectroscopy (FTIR) technique in order to reveal functional groups. Good adsorption characteristics can be attributed to presence of carboxyl, lactone, carbonyl, hydroxyl, sulfonate, and other surface functional groups in biosorbents which can act as binding sites for pollutants [19].

Adsorption characteristics of mentioned biosorbents were examined and discussed on the basis of experimental data of methylene blue (MB) uptake from aqueous solutions. MB is a thiazine cationic dye and has widespread applications for coloring paper, hair, cottons, and wools [20]. It is also used in microbiology, surgery, and diagnostics and as a sensitizer in photo-oxidation of organic pollutants and coating for paper stock. Due to its low toxicity, it cannot cause serious harmful effects in humans [20]. However, in high concentration, it causes heartbeat increase, vomiting, shocks, cyanosis, jaundice, and tissue necrosis [20]. In this paper, MB was used as a model of cationic pollutant in water systems.

Kinetics of adsorption was studied by fitting experimental data with four widely applied kinetics models: pseudo-first-order, pseudo-second-order, Elovich's model, and intraparticle diffusion kinetic model. Equilibrium adsorption data were fitted by Langmuir, Freundlich, and Dubinin–Radushkevich isotherm model. The efficiency of biosorbents, estimated by comparing the experimental adsorption data for MB, is as follows: *cc*LVB > *a*LVB > *r*LVB. These results indicate that chemical activation and modification are useful methods for improving adsorption characteristics of raw biosorbent based on *L. vulgaris* fruit shell. The results obtained in this study examining all biosorbents show a great potential for their application in the removal of cationic pollutants from aqueous solutions. Due to good adsorption characteristics, they can be used as filing in columns and reactors for water purification.

2. Materials and methods

2.1. Preparation of rLVB

L. vulgaris is a creeping, hardy plant which belongs to the *Cucurbitaceae* family. The fruit shell is recognized to be hard and ligneous covering the spongy white pith characterized by bitter taste. Fresh biomass of *L. vulgaris* fruit was collected in the south area of Serbia (near the City of Niš) at about 200 m altitude. Plants were grown under controlled conditions with irrigation and without fertilization. All planted at the same time in mid-April and harvested in the mid-October, also all at the same time.

For preparation of raw biosorbent material based on *L. vulgaris*, naturally dried fruit shell was washed a few times with distilled and deionized water, roughly crushed, and grounded by laboratory mill (Waring, Germany). After drying in the oven at 55 ± 5°C to constant weight, biomass was fractionized, using standard sieves (Endecotts, England), to obtain particle sizes ranging from 0.8 to 1.25 mm, which was used for batch adsorption studies and further characterizations. The obtained biosorbent was stored in an air-tight plastic container and denoted as *r*LVB for convenience.

2.2. Preparation of aLVB

Obtained rLVB was soaked in 0.3 M HNO_3 for 24 h to remove metals bio-accumulated in the plant during growing. After that, biomass was washed with

deionized water to remove excess acid and treated with 0.1 M NaOH in period of 30 min. Excess alkali was removed by thoroughly washing with deionized water and biomass was dried at 55 ± 5°C to constant weight. The prepared adsorbent was denoted as activated *L. vulgaris* biosorbent (*a*LVB) and stored in an air-tight plastic container.

2.3. Preparation of ccLVB

For *cc*LVB preparation, concentrated sulfuric acid was gradually added to the raw biosorbent and temperature of the mixture was held at 40°C for 2 h by water bath. At the end of 2 h, mixture was diluted by sufficient amount of deionised water and then was filtrated. In order to remove remaining sulfuric acid, the biosorbent was washed several times with deionised water over a Büchner funnel, until the filtrate did not give precipitate with barium—chloride. After that, biosorbent was neutralized by adding small portions of 0.1 M NaOH untill pH reached 6.5–7.0. Finally, biosorbent was filtered, dried in a oven at 55 ± 0.5°C, and stored in polyethylene tubes for further experimental use. Obtained black material was denoted as "cold carbonized" *L. vulgaris* biosorbent (*cc*LVB).

2.4. FTIR characterization

FTIR spectroscopy characterization was carried out for an analysis of major functional groups of raw and functionalized biosorbent samples. FTIR spectra were recorded by means of BOMEM MB-100 FTIR spectrometer (Hartmann & Braun, Canada) using KBr pellets containing 1 mg of the sample in 150 mg KBr. Instrument is equipped with a standard DTGS/KBr detector in the range of 4,000–400 cm^{-1} with a resolution of 2 cm^{-1}. Biosorbents were dried at 110°C before FTIR analysis.

2.5. The pH of biosorbents

The pH of the biosorbents was measured after stirring overnight in a suspension containing 0.2 g of biosorbent added to 50 cm^3 of deionised water.

2.6. Boehm titrations

Titrations were carried out in Erlenmayer flasks at 20°C under nitrogen in order to avoid dissolution of carbon dioxide in the solution [21,22]. First, each biosorbent was protonated with 0.01 M HCl, and dried at 50°C. Then, 0.5 g of protonated biosorbent was suspended in 50 cm^3 of a 0.1 M $NaNO_3$. In order to achieve equilibrium, suspension was stirred on magnetic stirrer for 1.5 h prior to titration. Increments of base (0.04–0.06 cm^3) were successively added. Next increment was added after reaching equilibrium.

2.7. Effect of contact time on biosorption

All biosorption experiments were carried out in duplicate or triplicate under the batch conditions and results are given as arithmetic mean values. Working solutions of MB dye (CI 52015) were prepared by diluting the stock solution, concentration of 1,500 mg dm^{-3}, with deionised water to the needed concentration. Fresh dilutions were used for each adsorption study. Initial pH of solutions was adjusted to 5.0 ± 0.1 pH, metrically with 0.1 and 0.01 M HCl or NaOH, without buffering.

Experiments were conducted in 400 cm^3 Erlenmeyer flasks, using 250 cm^3 of the dye model solution. Flasks were stirred at 250 rpm at the required temperature. Batch biosorption tests were done at different contact time at the initial concentration of MB 50 mg dm^{-3} and biosorbent dose of 2.0 g dm^{-3} in 250 cm^3 solution. The temperature was controlled at 22°C. Aliquots of solutions (5.0 cm^3) were withdrawn at preset time intervals; the biosolids were removed immediately by a filtration through a 0.45 μm regenerated cellulose membrane filter (Agilent Technologies, Germany). The concentration of MB in solution after proper dilution was determined using a UV–vis spectrophotometer (Shimadzu UV-1,650 pc) by measuring the absorbance at a wavelength of 660 nm. Kinetic experiments were performed by taking samples in the defined intervals up to 180 min.

2.8. Equilibrium adsorption studies

Sorption studies were conducted in a routine manner by the batch technique in 250 cm^3 Erlenmeyer flasks containing 100 cm^3 of dye solutions. The flasks were continuously stirred on magnetic stirrer for 120 min to ensure that equilibrium was reached. Before analysis, the samples were filtered as described above and the supernatant fraction was analyzed for the remaining dye ions. Adsorption studies were performed at a constant temperature of 22°C and initial pH 5.0 ± 0.1. All the biosorption experiments were repeated thrice to confirm the results. The data were the mean values of three replicated determinations. The uptake of dye by unit mass of biosorbent at any time (q) was determined from Eq. (1):

$$q_e = \frac{V(C_0 - C_e)}{m_{ads}} \quad (1)$$

in which V is the volume of MB solution (dm^3), C_0 is the initial concentration of the MB solution ($mg\,dm^{-3}$), C_e is the equilibrium concentration of the MB solution ($mg\,dm^{-3}$), and m_{ads} is the mass of adsorbent (g).

2.9. Effect of pH on MB adsorption

Effect of pH was examined using 100 cm^3 dye solutions, concentration of 100 $mg\,dm^{-3}$, and biosorbent dosage of 2.0 $g\,dm^{-3}$. The dye solutions were adjusted to the initial pH values of 2, 3, 5, 6, and 7 by HCl or NaOH. After adding biosorbent, suspensions were stirred for 120 min at 22°C on a magnetic stirrer operating at 200 rpm.

3. Results and discussion

3.1. FTIR analysis

Peaks appearing in the FTIR spectrum of *r*LVB and *a*LVB (Fig. 1) are assigned to various groups and bonds in accordance with their respective wavenumbers (cm^{-1}) as reported in the literature [14,23–27].

In the FTIR spectrum of *r*LVB, the broad and intense peak at around 3,416 cm^{-1} (ranging from 3,200 to 3,600 cm^{-1}) is assigned to the stretching of O–H group due to inter and intramolecular hydrogen bonding of polymeric compounds, such as alcohols, casually phenols, and carboxylic acids presented in the already-proved cellulose and lignin. The O–H stretching vibrations result within a range of wavenumbers specifying the presence of bonded O–H of carboxylic acids and/or free hydroxyl groups [24,28]. The band at near 2,924 cm^{-1} indicates symmetric and/or asymmetric C–H stretching vibration of aliphatic acids. Similarly, the peak observed at 2,855 cm^{-1} is assigned to the symmetric stretching vibration of CH_2 due to C–H bonds of additionally proved aliphatic acids in such biosorbent [29]. The clear peak registered at 1,738 cm^{-1} represents the stretching vibration of C=O bond, which may originate from nonionic carboxyl groups (–COOH, $–COOCH_3$), and may be denoted to carboxylic acids or corresponding esters. Asymmetric and symmetric stretching vibrations of ionic carboxyl groups from carboxylate salts ($–COO^-M^+$) appeared at 1,636 and 1,458 cm^{-1} [14,24]. Moreover, intense band at 1,048 cm^{-1} can be connected with the existence of stretching vibration of C–OH of alcoholic groups and already-registered carboxylic acids [29].

FTIR spectrum of *a*LVB is more or less similar to that of the *r*LVB characterized with changes in reduction of band intensities. Moreover, it can be clearly seen that peak at 1,738 cm^{-1} is weaker for *a*LVB than in the case of *r*LVB and disappear in *cc*LVB spectrum. This confirms the fact that carboxyl groups of *a*LVB and *cc*LVB are mostly in ionic form due to hydrolysis of –COOR and ionization of –COOH. Moreover, FTIR spectra confirm ligno-cellulose composition of *r*LVB and *a*LVB biosorbents. The most prominent cellulose bands in the *r*LVB and *a*LVB spectra between 1,000

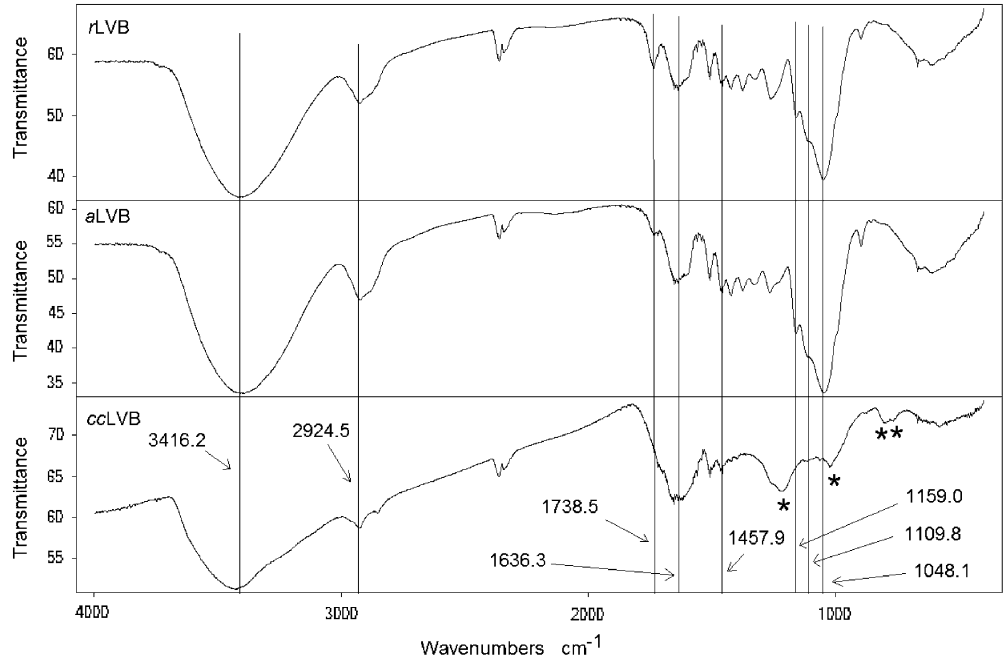

Fig. 1. FTIR spectra of *L. vulgaris*-based biosorbents: *r*LVB, *a*LVB, and *cc*LVB.

and 1,200 cm^{-1} can be observed at 1,048, 1,110, and 1,159 cm^{-1}, while the major diagnostic lignin bands can be identified at approximately 1,221, 1,269, 1,326, 1,367, 1,423, 1,464, 1,510, and 1,596 cm^{-1} [27].

Distinct changes in the FTIR spectrum are noted after sulfuric acid treatment of the native biosorbent. It is evident, when studying Fig. 1 that the main features of the "cold carbonized" biosorbent are bands around 1216.9, 1023.6, 802.3, and 765 cm^{-1} marked with asterix in the spectrum corresponding to *cc*LVB. New peak at 1216.9 cm^{-1} arises due to asymmetrical stretch of S=O bonds, while the other three bands confirms S–O vibrations. Hence, the appearance of sulfonate groups in the sulfuric-acid treated biosorbent is identified by the presence of mentioned vibrations in the spectrum. Moreover, peak corresponding to C–O stretching vibrations at ca 1,048 cm^{-1} is much weakened, while the band that corresponds to O–H stretching vibration is broadened and shifted to higher wavenumbers. These results indicate that the *cc*LVB possesses a small amount of hydroxyl groups, but dominantly sulfonate and carboxylic. Observed O–H vibrations originate mostly from adsorbed water molecules. Broadening and shifting of the O–H stretching vibrations can be attributed to an increase in the polydispersity in the modes of interaction of hydroxyls with their immediate surroundings, as a result of the major alterations in the self-assembled structures of cellulose. Additionally, it is worth to note that sulfuric acid treatment of *L. vulgaris* biomass induces dehydration and chemical changes similar to those that take place during the pyrolysis of lignin and cellulose [27]. Such modification causes an alteration of the raw biosorbent spectrum related to the reduction in the relative intensities of the cellulose bands after sulfuric acid treatment of raw biomass. Moreover, many lignin bands seen in the region 1,200–1,600 cm^{-1} have been lost in the *cc*LVB spectrum.

Based on the above analysis, it is clear from the FTIR spectra that the abundance of hydroxyl, carboxyl, and sulfonate groups are present at the *L. vulgaris*-based biosorbents. These groups may be involved in the coordination and ion-exchange reaction between surface and heavy metals [19,30], leading to their elimination from solutions.

3.2. The pH of biosorbents and potentiometric titrations

Initial pH value of distilled water is changed when it comes into contact with biosorbents. The pH value of 7.32 reveals weak basic surface characteristics of *r*LVB, while *a*LVB gives pH 6.90 which is almost unchanged pH value of distilled water. The most pronounced changes in pH are noticed for *cc*LBV which gives pH 5.65, probably due to presence of surface acidic groups. Fig. 2 shows the potentiometric titration curves of the protonated LVBs.

Similar curves were obtained for the all examined biosorbents but with different equivalence volumes. The titration curves obtained for *cc*LVB by the addition of $NaHCO_3$ solution have presented two dis-

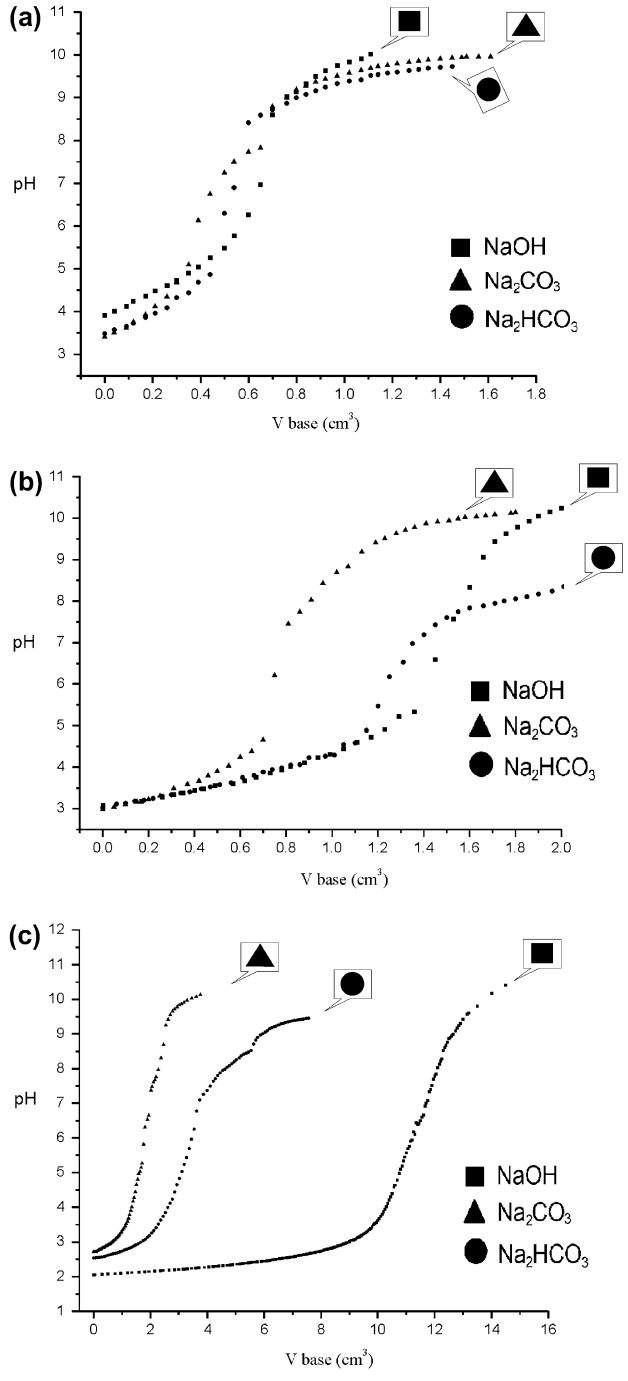

Fig. 2. Potentiometric titrations of the protonated (a) *r*LVB, (b) *a*LVB, and (c) *cc*LVB by base solutions of 0.1 M.

Table 1
Estimation of acidic functional groups on the sorbents by Boehm titrations

Type of surface groups	*r*LVB	*a*LVB	*cc*LVB
Strong acidic groups – carboxylic groups (mmolg^{-1})	0.104	0.275	0.725
Weak acidic groups – lactonic groups (mmolg^{-1})	0.218	0.160	0.353
Very weak acidic groups – phenolic groups (mmolg^{-1})	0.138	0.300	0.344

tinct waves showing the presence of two kinds of acidic groups, probably of carboxylic type. The equivalence points are located precisely by employing the first or second derivative of the experimental data. The quantitative estimations of the functional groups are given in Table 1 for all the biosorbents tested. These results reflect the changes induced by the overall chemical treatments. As can be seen from Table 1, concentration of strong acid groups increases after acid–base treatment of raw biomass during *a*LVB obtaining, especially after sulfuric acid treatment in the case of *cc*LVB. Such experimental data can be explained by hydrolysis of esters leading to formation of surface carboxyl. For the same reason, new phenolic –OH groups are formed resulting in increased concentration of very weak acidic groups.

3.3. Biosorption kinetics and modeling

The adsorption kinetics of MB dye removal onto *L. vulgaris*-based biosorbents are shown in the Fig. 3 by plotting the MB uptake per unit mass of biosorbent (q_t) vs. time (t).

In the case of *cc*LVB, a rapid initial adsorption leads to equilibrium within 25 min and the equilibrium period is then followed by a longer period of much slower uptake observed as plateau on the plot. For *r*LVB and *a*LVB, the adsorption process is more time consuming and nearly reaches equilibrium after 90 and 120 min, respectively. Four adsorption kinetic models have been used to examine and understand the adsorption mechanism and rate-limiting step. These include pseudo-first-order and pseudo-second-order rate model, Elovich's model, and intraparticle diffusion model [31,32], as shown in Fig. 4. Predicting the rate of adsorption for a given system is among the most important factors in adsorption system design, as the system's kinetics determines adsorbate residence time and the reactor dimensions. The validity of the exploited models is verified by the correlation coefficient, r^2.

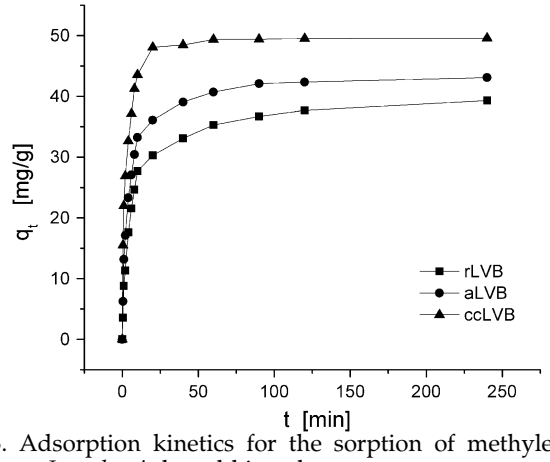

Fig. 3. Adsorption kinetics for the sorption of methylene blue onto *L. vulgaris*-based biosorbents.

Table 2 shows the adsorption kinetics parameters of pseudo-first-order and pseudo-second-order kinetic models. It is observed that both pseudo-first-order and pseudo-second-order kinetics possess high correlation coefficient values of 0.85–0.99 for all biosorbents.

By considering Fig. 4(a), it seems reasonable to assume that we may have to deal with a two-step kinetic process. A first fast initial kinetics is next followed by the slower kinetics, which corresponds to the second linear Lagergren plots in Fig. 3. The data belonging to first linear portions are far from equilibrium, so they cannot be correlated by the Lagergren equation. Hence, this procedure of linear regression can be used only for those C_t data points that were close to the equilibrium value C_e (in this case, such a situation is observed for the contact times higher than 20 min). Second kinetic process, for which pseudo-first-order constants are collected in Table 2, starts to dominate when about 77, 84, and 88% of the equilibrium dye amount is adsorbed onto *r*LVB, *a*LVB, and *cc*LVB, respectively. Based on high correlation coefficients for pseudo-first-order kinetics model, it can be concluded that the adsorption process of MB onto *r*LVB and *a*LVB is governed by the rate of adsorption reactions occurring at the solid/liquid interface. The fact that the correlation coefficient for *cc*LVB is lower than in the case of previous two suggests that adsorption kinetic is not dominantly under surface reaction control, but is rather of a diffusional character.

As can be seen, the Table 2 data indicate that the $q_{e,cal}$ values for the pseudo-second-order model

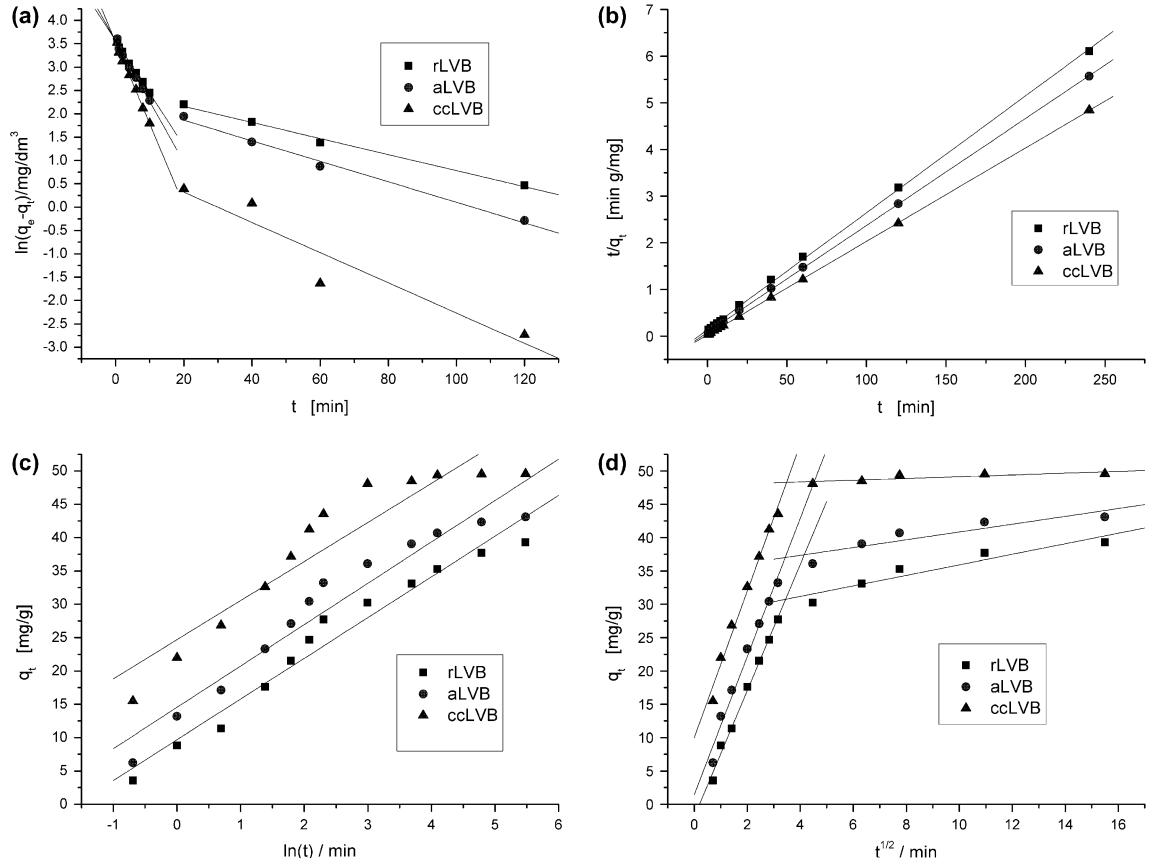

Fig. 4. (a) Pseudo-first-order, (b) pseudo-second-order, (c) Elovich, and (d) intraparticle diffusion kinetics for the sorption of methylene blue onto *L. vulgaris*-based biosorbents.

Table 2
Pseudo-first-order and pseudo-second-order kinetic constants for the sorption of methylene blue onto *L. vulgaris*-based biosorbents

Biosorbent	$q_{e,exp}$ (mg g^{-1})	Pseudo-first-order kinetics			Pseudo-second-order kinetics		
		$q_{e,cal}$ (mg g^{-1})	k_1 (min^{-1})	r^2	$q_{e,cal}$ (mg g^{-1})	k_2 (g mg^{-1} min^{-1})	r^2
*r*LVB	39.3	12.231	0.0172	0.9909	39.9	0.00452	0.9995
*a*LVB	43.1	9.994	0.0220	0.9882	43.6	0.00656	0.9999
*cc*LVB	49.6	2.635	0.0324	0.8522	49.9	0.01415	0.9999

are more close to $q_{e,exp}$ values in comparison to the pseudo-first-order values. As such, it can be concluded that MB sorption onto the biosorbent seems to be more appropriately represented by pseudo-second-order model implying that chemisorption is the rate-controlling step which involves valence forces through the sharing or exchange of electrons between the adsorbate and the surface of the adsorbent.

Complete elucidation of the adsorption kinetics is provided by the additional two models, as follows. The kinetic rate constants obtained from Elovich's and intraparticle diffusion kinetic model are given in Table 3.

Although the Elovich equation describes the kinetics of the chemisorption process, it has proved suitable for highly heterogeneous solid surfaces. This model best fits adsorption data for *r*LVB implying its ligno-cellulose structure with heterogeneous surface. Acid–base activation and sulfuric acid treatment make surface more uniform and as a result, correlation coefficients are lower indicating again that surface reaction is not rate determining step for MB adsorption onto *cc*LVB.

Table 3
Elovich and Intraparticle diffusion kinetic constants for the sorption of methylene blue onto *L. vulgaris*-based biosorbents

	Elovich kinetics			Intraparticle diffusion		
Biosorbent	α (mg g^{-1} min^{-1})	β (g mg^{-1})	r^2	k_i (mg g^{-1} min$^{-0.5}$)	Intercept	r^2
*r*LVB	7.697	0.164	0.9603	9.465	−1.878	0.9908
*a*LVB	2.368	0.161	0.9348	10.364	1.436	0.9753
*cc*LVB	1.249	0.171	0.8651	10.990	9.985	0.9816

The uptake of adsorbate to the adsorbent is carried out by transfer of mass from the adsorbate to adsorbent. A number of steps take place in this process. Usually, mechanism of dye removal from the solutions involved four steps; (1) migration of dye molecules from bulk solution to the surface of the adsorbent; (2) diffusion through the boundary layer to the surface of the adsorbent; (3) adsorption at a site; and (4) intraparticle diffusion into the interior of the adsorbent [33].

Previous studies by various researchers showed that the plot of q_t vs. $t^{1/2}$ represents multi linearity, which characterizes the two or more steps involved in the sorption process [18]. From Fig. 4(d), it was noted that the sorption process involves two phases including an initial linear portion (up to $\sqrt{t} < 3.45$) and a final second portion ($3.45 < \sqrt{t}$). Initial linear portion attribute to the intraparticle diffusion effect, while the second stage may be regarded as the diffusion through smaller pores, which is followed by the establishment of equilibrium. The first linear portion of the curves does not have zero intercepts (Fig. 4(d)) indicating that MB removal on biosorbents is complex. Intraparticle diffusion may be involved in the adsorption process but it may not be the controlling factor in determining the kinetics of the process. The slope of the first linear portion of the plot has been defined as the intraparticle diffusion parameter k_i (Table 3). On the other hand, the intercept of the plot reflects the boundary-layer effect. The larger the intercept, the greater the contribution of the surface sorption in the rate-limiting step. When the plots do not pass through the origin, this is indicative of some degree of boundary-layer control and this further show that the intra-particle diffusion is not the only rate-limiting step, but also other kinetic models may control the rate of adsorption, all of which may be operating simultaneously.

3.4. Adsorption isotherms

The experimental equilibrium data of MB adsorption onto *L. vulgaris* biosorbents were fitted to the three widely used isotherms Freundlich, Langmuir, and Dubinin–Radushkevich isotherms by linear method (Fig. 5). The calculated isotherm parameters are given in Table 3. Langmuir constant, q_m, represents the monolayer saturation at equilibrium, while the other Langmuir constant, K_L, indicates the affinity for the binding of adsorbate (MB). The order of K_L values for *L. vulgaris* biosorbents was found as: *r*LVB < *a*LVB << ccLVB, indicating a higher affinity of chemically modified biosorbents than *r*LVB. Value of R_L which is in the range 0–1 confirms the favorable MB adsorption process. MB is cationic dye with a heterocyclic aromatic molecule of planar three-ring structure. Such characteristics of MB molecule ensure pronounced adsorbability to the positively charged surfaces of biosorbents.

The Freundlich model does not describe the saturation behavior of the biosorbents. From Table 3, all obtained K_F values show higher MB adsorptive capacity of acid–base activated and sulfuric acid-treated biosorbent than its raw form. On average, a favorable adsorption tends to have Freundlich constant n between 1 and 10.

As stated in the literature, the E value of Dubinin–Radushkevich equation ranges from 1.0 to 8.0 kJ mol^{-1} for physical adsorption and from 8.0 to 16.0 kJ mol^{-1} for chemical ion-exchange adsorption [4]. Hence, it is possible to say that the mechanism of MB uptake on the biosorbents can be explained with a physical adsorption process (i.e. van der Waals forces). The E values confirm already-established order of biosorbent affinity to MB: *r*LVB < *a*LVB < *cc*LVB. The Dubinin–Radushkevich equation has shown a better fit to experimental data than Freundlich equation, but the best fit is in the case of Langmuir equation. In addition, it can be easily noticed that experimental adsorption data of *cc*LVB correlate well with all applied theoretical adsorption models (Table 4).

Acid–base activation of raw biomaterial resulted in the exposure of certain chemical groups, which enhanced the binding of cationic species. Namely, the pretreatment could cause hydrolysis of esters providing new reactive sites and increase of MB biosorption.

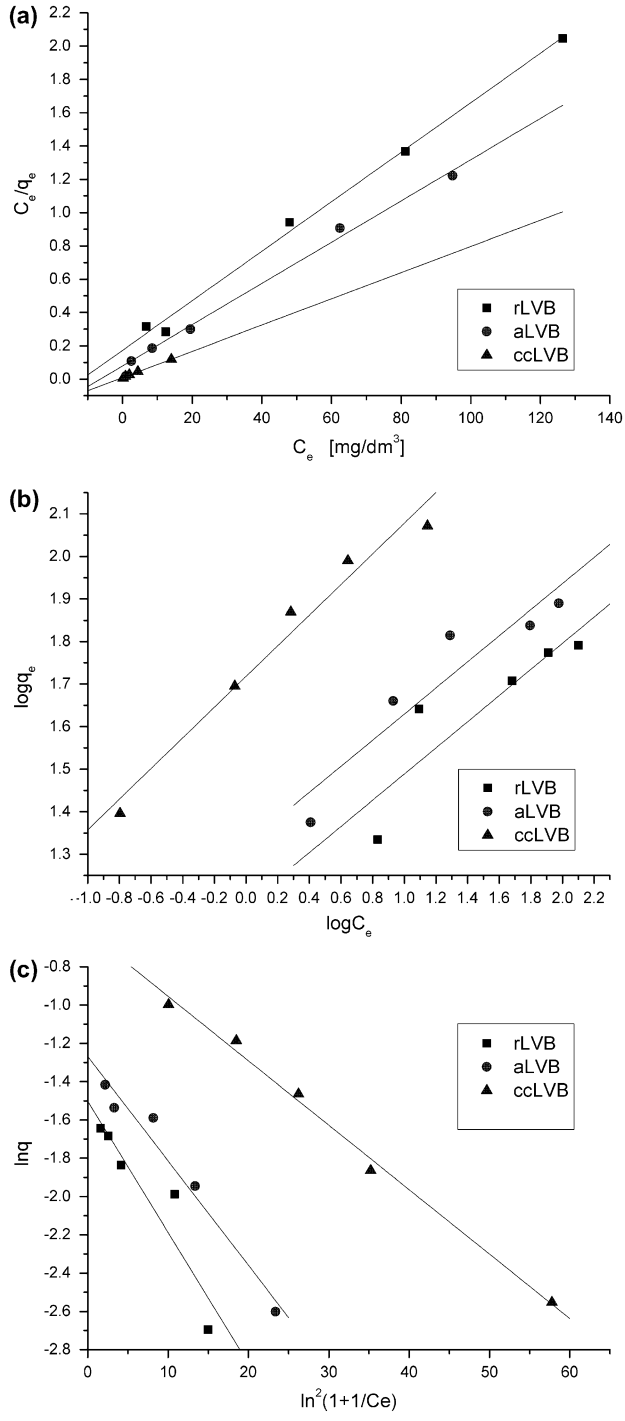

Fig. 5. (a) Langmuir, (b) Freundlich, and (c) Dubinin–Radushkevich isotherm plots for MB removal using *L. vulgaris* based biosorbents.

The introducing of new functional groups by sulfuric acid-treatment method such as $-SO_3^-$ contributes to the highest adsorbtion activity of *cc*LVB compared to *r*LVB and *a*LVB. In addition to van der Waals forces, the mechanism of MB removal from the solution probably involves hydrogen bonds and ion-exchange.

Table 4
Isotherm constants for the sorption of methylene blue onto *L. vulgaris*-based biosorbents

Isotherm	*r*LVB	*a*LVB	*cc*LVB
Langmuir			
q_m (mg g^{-1})	67.25	80.71	126.9
K_L (mg^{-1})	5.77	12.65	111.11
R_L	0.32–0.70	0.025–0.11	0.0045–0.022
r^2	0.9938	0.9938	0.9963
Freundlich			
K_F (l mg^{-1})	15.17	21.02	52.21
n	3.25	3.25	2.77
r^2	0.7356	0.8457	0.9594
Dubinin–Radushkevich			
q_m (mg g^{-1})	71.23	89.97	172.46
E (kJ mol^{-1})	2.70	3.03	3.85
r^2	0.8253	0.9564	0.9912

3.5. Effect of solution pH on biosorption

The pH value of the solution was an important controlling parameter in the adsorption process. Fig. 6 shows the effect of solution pH on values of q_e at the initial concentration of MB 100 mg dm^{-3}. In the case of *r*LVB and *a*LVB, it was observed that the values of q_e was minimum at the initial pH 2 and increased very sharply with the pH in the pH range from 2 to 5. While, when the value of pH was from 5 to 7, the adsorption quantity almost had no change. Therefore, pH 5 was chosen for the study on the effect of contact time and initial concentration of MB. Several reasons

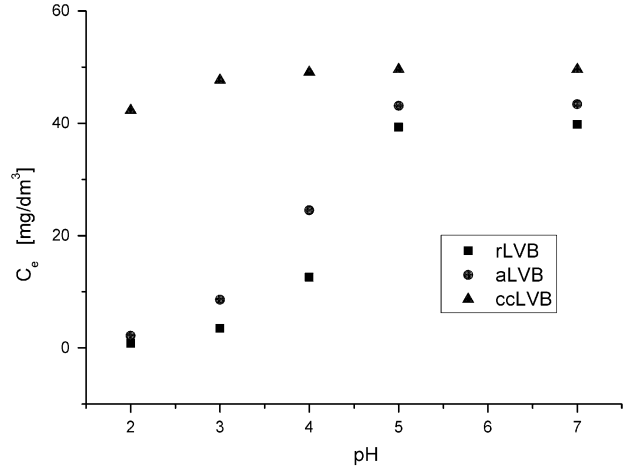

Fig. 6. Effect of pH on the uptake of MB onto LVBs.

Table 5
Adsorption results of MB by various biosorbents from the literature

Biosorbent	pH	t (°C)	Adsorption capacity mg g^{-1}
CNT [9]	7	25	46.2
Rice husk [11]	8	32	40.59
Yellow passion fruit peel [14]	8	25	44.70
Marine seaweed: *Caulerpa racemosa var. cylindracea* [16]	7	18	5.23
Polysulfone-immobilized *Corynebacterium glutamicum* [18]	8	22	166.5
Rhizopus arrhizus in the absence of surfactant (SDS) [20]	10	25	370.3
Fallen phoenix tree's leaves [34]	7	22	80.9

may be attributed to MB adsorption behavior of the sorbent relative to solution pH. At lower pH values, the surface of adsorbent would also be surrounded by the hydrogen ions, which compete with MB ions binding the sites of the sorbent. At higher pH, the surface of particles may get negatively charged, which enhances the positively charged dye cations through electrostatic forces of attraction. The percentage sorption of MB was not significantly altered when the initial pH was increased from 5 to 7. All proposed explanations are consistent with the fact that carboxyls are little or not at all ionized at pH 4, as this pH is close to the carboxylic acid's pKa.

Existence of strongly acidic groups ($-SO_3^-$) on the surface of *cc*LVB causes only a slight change in adsorption capacity with decreasing pH.

The maximum MB adsorption capacity, q_{max}, in the present study was compared with the other biosorbents reported in the literature (Table 5).

4. Conclusion

The *L. vulgaris*-based biosorbents denoted as *r*LVB, *a*LVB, and *cc*LVB are low-cost materials that can be used as alternative biosorbents for removal of the cationic pollutants from water. The biosorbents were characterized by FTIR spectroscopy indicating the dominant presence of –COOH, C–O, and O–H groups in *r*LVB and *a*LVB, while $-SO_3^-$ groups are confirmed in sulfuric acid-treated sample.

The contact time required for establishing equilibrium adsorption of MB onto *r*LVB, *a*LVB, and *cc*LVB was found to be 120, 90, and 25 min, respectively. The pseudo-second-order model described the biomass-MB kinetic data with the highest correlation coefficient indicating dominant chemisorption mechanism. In addition to chemisorption, significant contribution to the MB uptake has physisorption (i.e. van der Waals forces), hydrogen bonds, and ion-exchange. The theoretical monolayer saturation capacities of the *r*LVB, *a*LVB, and *cc*LVB for adsorption of MB, according to Langmuir model, were 67.25, 80.71, and 126.90 mg g^{-1}. The uptake of MB per mass of biosorbents depended greatly on pH. The optimum pH for the adsorption of MB onto *r*LVB and *a*LVB was in the range from 5 to 7, while MB adsorption onto *cc*LVB almost does not depend on pH.

With the advantages of being an inexpensive and easily available agricultural product, *L. vulgaris* biomass shows promising potential for the development of a practical biosorbent. In addition, it was shown that *r*LVB adsorption affinity to MB can be significantly enhanced via acid–base activation and sulfuric acid treatment.

Acknowlegement

The research was supported by the Serbian Ministry of Education and Science (Grant No. TR34008).

References

[1] V.K. Gupta, V.K. Saini, N. Jain, Adsorption of As(III) from aqueous solutions by iron oxide-coated sand, J. Colloid Interface Sci. 288 (2005) 55–60.
[2] N. Rajic, Dj. Stojakovic, S. Jevtic, N. Zabukovec-Logarb, J. Kovac, V. Kaucic, Removal of aqueous manganese using the natural zeolitic tuff from the Vranjska Banja deposit in Serbia, J. Hazard. Mater. 172 (2009) 1450–1457.
[3] M. Ranđelović, M. Purenović, A. Zarubica, J. Purenović, I. Mladenović, G. Nikolić, Alumosilicate ceramics based composite microalloyed by Sn: An interaction with ionic and colloidal forms of Mn in synthetic water, Desalination 279 (2011) 353–358.
[4] M. Ranđelović, M. Purenović, A. Zarubica, J. Purenović, B. Matović, M. Momčilović, Synthesis of composite by application of mixed Fe, Mg (hydr)oxides coatings onto bentonite—A use for the removal of Pb(II) from water, J. Hazard. Mater. 199–200 (2012) 367–374.
[5] T.K. Naiya, A.K. Bhattacharya, S.K. Das, Adsorption of Cd(II) and Pb(II) from aqueous solutions on activated alumina, J. Colloid Interface Sci. 333 (2009) 14–26.
[6] L. Wang, J. Zhang, R. Zhao, C. Li, Y. Li, C. Zhang, Adsorption of basic dyes on activated carbon prepared from *Polygonum orientale Linn*: Equilibrium, kinetic and thermodynamic studies, Desalination 254 (2010) 68–74.
[7] S.Z. Mohammadi, M.A. Karimi, D. Afzali, F. Mansouri, Removal of Pb(II) from aqueous solutions using activated carbon from Sea-buckthorn stones by chemical activation, Desalination 262 (2010) 86–93.

[8] M. Momčilović, M. Purenović, A. Bojić, A. Zarubica, M. Ranđelović, Removal of lead(II) ions from aqueous solutions by adsorption onto pine cone activated carbon, Desalination 276 (2011) 53–59.
[9] Y. Yao, F. Xu, M. Chen, Z. Xu, Z. Zhu, Adsorption behavior of methylene blue on carbon nanotubes, Bioresour. Technol. 101 (2010) 3040–3046.
[10] M.M. Jadhao, L.J. Paliwal, N.S. Bhave, Ion-exchange properties of 2,2′-dihydroxybiphenyl–urea–formaldehyde terpolymer resins, Desalination 247 (2009) 456–465.
[11] V. Vadivelan, K.V. Kumar, Equilibrium, kinetics, mechanism, and process design for the sorption of methylene blue onto rice husk, J. Colloid Interface Sci. 286 (2005) 90–100.
[12] M. Sciban, B. Radetic, Z. Kevresan, M. Klasnja, Adsorption of heavy metals from electroplating wastewater by wood sawdust, Bioresour. Technol. 98 (2007) 402–409.
[13] A. Witek-Krowiak, R.G. Szafran, S. Modelski, Biosorption of heavy metals from aqueous solutions onto peanut shell as a low-cost biosorbent, Desalination 265 (2011) 126–134.
[14] F.A. Pavan, E.C. Lima, S.L.P. Dias, A.C. Mazzocato, Methylene blue biosorption from aqueous solutions by yellow passion fruit waste, J. Hazard. Mater. 150 (2008) 703–712.
[15] C. Namasivayam, D. Prabha, M. Kumutha, Removal of direct red and acid brilliant blue by adsorption on to banana pith, Bioresour. Technol. 64 (1998) 77–79.
[16] S. Cengiz, L. Cavas, Removal of methylene blue by invasive marine seaweed: *Caulerpa racemosa var. cylindracea*, Bioresour. Technol. 99 (2008) 2357–2363.
[17] K.S. Low, C.K. Lee, K.K. Tan, Biosorption of basic dye by water hyacinth roots, Bioresour. Technol. 52 (1995) 79–83.
[18] K. Vijayaraghavan, J. Mao, Y.-S. Yun, Biosorption of methylene blue from aqueous solution using free and polysulfone-immobilized *Corynebacterium glutamicum*: Batch and column studies, Bioresour. Technol. 99 (2008) 2864–2871.
[19] D.-L. Mitic-Stojanovic, A. Zarubica, M. Purenovic, D. Bojic, T. Andjelkovic, A.Lj. Bojic, Biosorptive removal of Pb^{2+}, Cd^{2+} and Zn^{2+} ions from water by *Lagenaria vulgaris* shell, Water SA, 37(3) (2011) 303–312.
[20] Z. Aksu, S. Ertugrul, G. Donmez, Methylene Blue biosorption by *Rhizopus arrhizus*: Effect of SDS (sodium dodecylsulfate) surfactant on biosorption properties, Chem. Eng. J. 158 (2010) 474–481.
[21] M.E. Fernandez, G.V. Nunell, P.R. Bonelli, A.L. Cukierman, Batch and dynamic biosorption of basic dyes from binary solutions by alkaline-treated cypress cone chips, Bioresour. Technol. 106 (2012) 55–62.
[22] A.E. Ofomaja, E.B. Naidoo, Biosorption of lead(II) onto pine cone powder: Studies on biosorption performance and process design to minimize biosorbent mass, Carbohydr. Polym. 82 (2010) 1031–1042.
[23] N. Barka, M. Abdennouri, M. El Makhfouk, Removal of Methylene Blue and Eriochrome Black T from aqueous solutions by biosorption on Scolymus hispanicus L.: Kinetics, equilibrium and thermodynamics, J. Taiwan Inst. Chem. E 42 (2011) 320–326.
[24] M. Iqbal, A. Saeed, S.I. Zafar, FTIR spectrophotometry, kinetics and adsorption isotherms modeling, ion exchange, and EDX analysis for understanding the mechanism of Cd^{2+} and Pb^{2+} by mango peel waste, J. Hazard. Mater. 164 (2009) 161–171.
[25] K.K. Krishnani, M.X. Xiaoguang, C. Christodoulatos, V.M. Boddu, Biosorption mechanism of nine different heavy metals onto biomatrix from rice husk, J. Hazard. Mater. 153 (2008) 1222–1234.
[26] G.C. Panda, S.K. Das, A.K. Guha, Biosorption of cadmium and nickel by functionalized husk of *Lathyrus sativus*, Colloids Surf. B 62 (2008) 173–179.
[27] D.W. Rutherford, R.L. Wershaw, L.G. Cox, Changes in Composition and Porosity Occurring during the Thermal Degradation of Wood and Wood Components Scientific Investigations Report, U.S. Geological Survey (2005).
[28] R. Gnanasambandam, A. Protor, Determination of pectin degree of esterification by diffuse reflectance Fourier transform infrared spectroscopy, Food Chem. 68 (2000) 327–332.
[29] G. Guibaud, N. Tixier, A. Bouju, M. Baudu, Relation between extracellular polymers composition and its ability to complex Cd, Cu and Pb, Chemosphere 52 (2003) 1701–1710.
[30] A. Chergui, M.Z. Bakhti, A. Chahboub, S. Haddoum, A. Selatnia, G.A. Junter, Simultaneous biosorption of Cu^{2+}, Zn^{2+} and Cr^{6+} from aqueous solution by *Streptomyces rimosus* biomass, Desalination 206 (2007) 179–184.
[31] W.H. Cheung, Y.S. Szeto, G. McKay, Intraparticle diffusion processes during acid dye adsorption onto chitosan, Bioresour. Technol. 98 (2007) 2897–2904.
[32] H. Qiu, L. Lv, B. Pan, Q. Zhang, W. Zhang, Q. Zhang, Critical review in adsorption kinetic models, J. Zhejiang Univ. Sci. A 10(5) (2009) 716–724.
[33] S.M. El-Geundi, Color removal from textile effluents—by adsorption techniques, Water Res. 25 (1991) 271–273.
[34] R. Han, W. Zou, W. Yu, S. Cheng, Y. Wang, J. Shi, Biosorption of methylene blue from aqueous solution by fallen phoenix tree's leaves, J. Hazard. Mater. 141(1) (2007) 156–162.